Intern. J. Neuroscience, 1980, Vol. 10, pp. 145-164
0020-7454/80/1002-0145$04.50/0

PREDICTIONS AND PROPERTIES OF A MODEL OF POTASSIUM AND CALCIUM ION MOVEMENTS DURING SPREADING CORTICAL DEPRESSION

HENRY C. TUCKWELL

Department of Biomathematics, University of California, Los Angeles, Ca 90024, U.S.A.

(*Received July 19, 1979*)

A mathematical model for spreading depression, in which the movement of potassium ions and calcium ions is taken into account by means of a coupled system of reaction diffusion equations, is analysed. The effects of varying the parameters of the model are ascertained. These effects are analysed in terms of phase portraits. A critical point in the phase plane determines the minimum amplitude of the wave solutions. The position of this critical point relative to the trajectory on the solitary wave solution determines the shape of the wave profile. The model is found to predict wave profiles as observed experimentally. The model predicts a threshold K^+ concentration which is close to the observed threshold of 10 mM. When a stimulus of elevated K^+ is locally sustained, a train of SD waves emerges as in experiments where suprathreshold concentrations of potassium chloride are applied. Under some conditions it is impossible to elicit an SD wave. The relative values of the strengths of the pumps and other source terms determines the shape of the waves. A comparison of results from the model equations with data on TTX treated cat cortex yields satisfactory agreement between the amplitude and possibly the speed of the waves. For these small amplitude waves (less than about 25 mM) a linear relation between velocity and amplitude of the K^+ wave is found. Action potentials are included in the model by inserting an extra source term in the potassium equation, this being done in an approximate way which obviates the use of the Hodgkin–Huxley equations. When this is done waves of large amplitude (up to 100 mM) are obtained. It was found that treating the ratio of the presynaptic to extracellular volume differently from the ratio of the postsynaptic volume to the extracellular volume plays an important role in determining the amplitude of the response to locally elevated K^+ concentration. With the large amplitude waves a linear relationship is also found between velocity and amplitude. When the theoretical and experimental amplitude and time course of the K^+ wave are matched at a depth of 0.5 mm in rat cortex, the velocity predicted by the model is 2.9 mm/minute which compares favorably with the experimental value of 3 mm/minute. In other comparisons with experiment, the velocity is in the range of experimental velocities except in one case, cat cerebellum, where the predicted velocity is much smaller than the observed velocity. It is suspected, however, that the experimentally reported velocity may be too high, as it is based on indirect evidence. The questions not addressed by the model are discussed as are the successful predictions and the difficulties expected in obtaining reliable estimates of the magnitudes of the various source and sink terms for the ions in any cortical structure.

Spreading depression (SD) is a wave phenomenon that occurs in brain structures that are endowed with large proportions of gray matter. The SD wave, whose functional significance remains to be fully understood, may be instigated by various (apparently noxious) stimuli such as application of potassium chloride, electrical stimulation, mechanical pressure, etc. Its velocity of propagation is usually cited as being about 3 mm/min., with a range of 2–6 mm/min. (Ochs, 1962), but recent reports indicate velocities as small as 0.5 mm/min and perhaps as high as 9 mm/min. (Kraig & Nicholson, 1978). A fairly recent and very comprehensive source book of facts about SD has been compiled by Bures *et al.* (1974).

SD derived its name from its first experimentally observed effect, namely a localized transient depression of the recorded electroencephalographic activity which propagated from one part of the cortex to another (Leao, 1944). There is an accompanying slow surface negative wave of potential of amplitude about 15 mV, though sometimes this is preceded and/or followed by surface positivity. Neurons in the path of the SD wave usually cease their spiking activity and recent microelectrode recordings indicate that both

Davis Cope kindly provided a computer program for solving the reaction-diffusion equations. Betty Lang assisted in preparation of the manuscript. This work supported in part by NRC of Canada grants A4559 and A9259 to Robert Miura and Frederic Wan at the University of British Columbia.

neurons and glial cells undergo extensive depolarization (i.e., decreased potential difference across their membranes) as the SD wave passes (Higashida *et al.*, 1974; Sugaya *et al.*, 1975).

It was shown by Brinley *et al.* (1960) and Krivanek & Bures (1960) that SD was accompanied by an increase in extracellular potassium ion (K^+) concentration. Recent experiments have confirmed this (Vyskocil *et al.*, 1972) and indicated that there are concomitant decreases in the extracellular concentrations of sodium (Na^+), chloride (Cl^-) and calcium (Ca^{++}) ions (Nicholson *et al.*, 1977; Nicholson *et al.*, 1978; Kraig & Nicholson, 1978).

The mechanisms whereby SD is instigated and propagates are not yet understood. The first theoretical investigation was that of Grafstein (1956; 1963) who concluded that K^+ was the primary chemical in SD. An accumulation of K^+ in the extracellular space diffuses to neighbouring cortex thereby depolarizing nerve cells. The cells fire action potentials thereby releasing more K^+ which diffuses to uninvaded regions; thus the phenomenon propagates. A single reaction-diffusion equation was employed by Grafstein to model the concentration of K^+. Though this equation predicts the spread of K^+ there is no recovery process, the latter being inserted somewhat artificially.

There are a large number of chemicals which seem to play a role in SD. Amongst these are the four ions already mentioned along with neurotransmitter substances which cause membrane conductance changes for various ions. Many ions and organic molecules are involved in the metabolic processes which supply energy for the active transport of various substances against their concentration gradients (pumps). Modelling these active transport processes is extremely complicated in itself (Sachs, 1977) and a simple model for SD has been developed (Tuckwell & Miura, 1978) in which attention is focused on the concentrations of K^+, Ca^{++}, Na^+, Cl^- and excitatory and inhibitory transmitter substances. Other models of SD are possible but certain details of this first model seem to be sound as it predicts waves of diminished Ca^{++}, Cl^- and Na^+ and increased K^+ with concomitant cellular depolarization moving across the cortical structure at velocities in the range of experimental ones. A model has also been developed in which the transmitter substance (in particular glutamate) appears explicitly in the equations and this is expected to be useful in addressing the question mainly raised by Van Harreveld (Van Harreveld & Fifkova, 1973) as to which chemical (K^+ or glutamate) is the primary agent in SD. Details of this model will be published in the near future.

The aim of this investigation was to find which properties of SD waves in cortical structures are correctly predicted by the model to be described and to see how the model solutions depend upon the various parameters, all of which have well defined physiological and anatomical meaning.

THE MODEL EQUATIONS

The model equations to be employed are slightly different from those derived previously (Tuckwell & Miura, 1978). Attention here again focuses on K^+ and Ca^{++} as these ions apparently play important roles in SD, particularly in TTX treated cortex. Potassium ions are mainly responsible for the depolarization of neuronal (and glial) elements and calcium ions are believed to be important in the process of transmitter release.

We will consider the problem in one space dimension only as the essential phenomena can still then be obtained. Let $K^o(x,t)$, $K_1^i(x,t)$, $K_2^i(x,t)$, $Ca^o(x,t)$, $Ca_1^i(x,t)$ and $Ca_2^i(x,t)$ be the extracellular, postsynaptic intracellular and presynaptic intracellular concentrations, in mM/liter (abbreviation, mM) of potassium and calcium ions in the cortical tissue. The presynaptic elements (terminals, spines) are assumed to have a certain extent so that the ratio of the presynaptic volume to the extracellular volume is possibly different from the ratio of the postsynaptic volume to the extracellular volume. If glial cells were included, a third intracellular compartment would be included but this will not be done here.

The basic model equations can be written as reaction-diffusion equations for the extracellular concentrations with sources and sink terms which describe the fluxes into and out of the various intracellular compartments. The pre- and postsynaptic concentrations satisfy ordinary differential equations as diffusion in the intracellular compartments is neglected. We thus have:

$$\frac{\partial K^o}{\partial t} = D_K \frac{\partial^2 K^o}{\partial x^2} + F_1(\mathbf{C}) + F_2(\mathbf{C}), \qquad (1)$$

$$\frac{\partial K_1^i}{\partial t} = -\frac{\alpha}{\beta} F_1(\mathbf{C}), \qquad (2)$$

$$\frac{\partial K_2^i}{\partial t} = -\frac{\alpha}{\gamma} F_2(\mathbf{C}), \tag{3}$$

$$\frac{\partial Ca^o}{\partial t} = D_{Ca}\frac{\partial^2 Ca^o}{\partial x^2} + G_1(\mathbf{C}) + G_2(\mathbf{C}), \tag{4}$$

$$\frac{\partial Ca_1^i}{\partial t} = -\frac{\alpha}{\beta} G_1(\mathbf{C}), \tag{5}$$

$$\frac{\partial Ca_2^i}{\partial t} = -\frac{\alpha}{\gamma} G_2(\mathbf{C}) \tag{6}$$

where D_K and D_{Ca} are the diffusion coefficients of potassium and calcium ions in the extracellular space. The quantities α, β and γ represent the fractions of the total volume that are extracellular space, postsynaptic intracellular space and presynaptic intracellular space, with $\alpha+\beta+\gamma = 1$. The vector $\mathbf{C}$ in the arguments of all the reaction terms represents all the relevant ion concentrations.

We will deal first with the case of cortex treated with TTX. This chemical blocks sodium channels which are operative during action potential instigation and propagation, and one expects the ion fluxes during SD to be much reduced if action potentials are not present. This is supported by the one available set of experimental data on external K^+ concentration during SD in cat cerebral cortex treated with TTX (Sugaya *et al.*, 1975). The K^+ concentration normally rises to about 50 mM in this preparation but with TTX the increase is only to about 10 mM.

The ion concentrations to be incorporated in the equations to be solved are K^o, K_1^i, Ca^o and Ca_2^i. The reason for this is that the most important flux of K^+ will be out of postsynaptic membrane and the most important flux of Ca^{++} will be into presynaptic membrane. From now on we will drop the subscripts on the internal concentrations.

The system becomes a little more simple:

$$\frac{\partial K^o}{\partial t} = D_K\frac{\partial^2 K^o}{\partial x^2} + F(\mathbf{C}), \tag{7}$$

$$\frac{\partial K^i}{\partial t} = -\frac{\alpha}{\beta} F(\mathbf{C}), \tag{8}$$

$$\frac{\partial Ca^o}{\partial t} = D_{Ca}\frac{\partial^2 Ca^o}{\partial x^2} + G(\mathbf{C}), \tag{9}$$

$$\frac{\partial Ca^i}{\partial t} = -\frac{\alpha}{\gamma} G(\mathbf{C}). \tag{10}$$

The incorporation of β and γ which may take different values was found to be very important in determining the nature of the solutions.

The reaction terms under certain approximations are as derived previously and can be written:

$$F(\mathbf{C}) = -k_1(V-V_K)V - V_{Ca})g(V) - k_2\{1-\exp[-k_3(K^o-K_R^o)]\}, \tag{11}$$

$$G(\mathbf{C}) = k_4(V-V_{Ca})g(V) + k_5\{1-\exp[-k_6(Ca^i-Ca_R^i)]\}, \tag{12}$$

where k_i, $i = 1, 2, \ldots, 6$ are positive constants and K_R^o and Ca_R^i are the resting external K^+ concentration and resting presynaptic internal Ca^{++} concentration. The remaining quantities are the individual ion equilibrium potentials.

$$V_K = (RT/F)\ln(K^o/K^i), \tag{13}$$

$$V_{Ca} = (RT/2F)\ln(Ca^o/Ca^i), \tag{14}$$

and the membrane potential given by the Goldman–Hodgkin–Katz formula (Hodgkin & Katz, 1949),

$$V = (RT/F)\ln\left[\frac{K^o+p_{Na}Na^o+p_{Cl}Cl^i}{K^i+p_{Na}Na^i+p_{Cl}Cl^o}\right], \tag{15}$$

where R is the gas constant, T is the absolute temperature, F is Faraday's constant, Na^o, Na^i, Cl^o, Cl^i refer to the external and internal concentrations of Na^+ and Cl^- and p_{Na} and p_{Cl} are the membrane permeabilities of sodium and chloride ions relative to that of potassium ions. In all of the results to be presented here it is assumed that the variations in the concentrations of sodium and chloride are such that they do not have a large effect on V and hence can be taken to be at their resting values. This is reasonable because: (a) the changes in these ion concentrations (which are estimated to be of order 15 mM during SD with TTX treated cortex) affect V to less extent than those of K^+ and (b) the changes in sodium and chloride are in opposite directions in their effect on V and hence tend to cancel each other. Furthermore, results have been obtained in the more complicated system which permits changes in sodium and chloride concentrations and the basic phenomena of interest are changed very little (e.g., wave shapes, amplitudes and speed). It is

possible to obtain more insight with a system in which there are only two ions as components of the model because phase plane drawings are easy to comprehend as opposed to phase analysis in three or more dimensions. There is another simplifying assumption implicit in Eqs. (11) and (12) which is that the membrane potentials of presynaptic and postsynaptic membrane are not distinguished.

The remaining quantity in the model equations is $g(V)$ which depicts the variation in presynaptic membrane calcium conductance with membrane potential. Available experimental evidence (Quastel, 1974; Llinas *et al.*, 1976) enables this to be satisfactorily represented by

$$g(V) = 1+\tanh[k_7(V+V_T)], \qquad (16)$$

where k_7 is a positive constant and V_T is a threshold-type voltage at which the value of the calcium conductance starts to become appreciable. In practice $g(V)$ is cut off close to resting conditions because the pump terms in (11) and (12) (those containing the exponentials) go to zero at resting levels. In numerical computation this was achieved by multiplying $g(V)$ by $H(K^o-K_*^o)$ where K_*^o is just greater than K_R^o, $H(\cdot)$ being the unit step function.

It is worth dwelling on the physiological and anatomical meaning of the constants k_1 through k_6. The factors which determine k_4 are the area of presynaptic membrane per unit volume of tissue and the calcium conductance per unit area of presynaptic membrane. The constant k_1 is also determined by these factors and in addition the "time for which released transmitter is effective" in producing a postsynaptic conductance change, the magnitude of this conductance change per unit area of postsynaptic membrane and the area of postsynaptic membrane per unit volume of cortex. If we assume that the active transport is occurring at actual "pump sites," then k_2 and k_5 contain the number of pump sites per unit area of membrane, the maximal pump rate for a single site and the area of membrane per unit volume. The values of k_3 and k_6 determine how great a departure from resting conditions will induce a maximal pump rate. The following terms will be employed: k_1 will be called the potassium source strength; k_2, the potassium pump strength; k_3, the potassium pump saturation rate; k_4, the calcium sink strength; k_5, the calcium pump rate; and k_6 the calcium pump saturation rate.

It is clear that none of the quantities $k_1, \ldots, k_6$ is known for any cortical structure, whereas most of the other parameters and constants are known to some extent. The approach is necessarily phenomenonological as certain values for the unknown constants are tried and the results ascertained.

There is another point worth raising and that is whether the relative permeabilities p_{Na} and p_{Cl} can be regarded as constants, as they are in the results to be presented. In the resting state these quantities are usually taken to have values 0.05 and 0.45 approximately though variations occur from preparation to preparation. It is known that during the spike p_{Na} increases and the Goldman–Hodgkin–Katz formula still gives about the right membrane potential (Brinley, 1963). The question becomes whether, during transmitter induced conductance changes which will effect changes in p_{Na} and p_{Cl} locally near the synapse, these changes should be incorporated into Eq. (15). This seems a fairly important matter but it seems that the overall qualitative behavior will not suffer much from the assumption that p_{Na} and p_{Cl} are constant. The study of this complication will also be deferred.

RESULTS AND DISCUSSION

The system of reaction-diffusion equations is integrated numerically given initial and boundary conditions. The numerical method employed was Lees' modification of the Crank–Nicolson scheme (Lees, 1969). The scaling in the computations was such that the spatial extent of the wave phenomena of interest occupied a relatively small fraction of the overall space interval. The boundary conditions were always such that at the ends of the interval the external potassium and calcium ion concentrations were at their resting values. The boundaries being remote from the wave phenomena means they have a negligible effect on the solutions. A simplification was made which enabled the system to be reduced to just two reaction–diffusion equations. The internal potassium ion concentration was held at resting level which is reasonable because its usual value is about 140 mM and its expected change is only to about 137.5 during SD in TTX treated cortex. Furthermore, calcium was taken to be "locally conserved" in accordance with,

$$Ca^i(x, t) = Ca_R^i + \frac{\alpha}{y}[C_R^o - C^o(x, t)], \qquad (17)$$

so that only one calcium concentration, $C^o(x,t)$, and one potassium concentration, $K^o(x,t)$, need be employed in the numerical calculations (Tuckwell, 1979). The use of relation (17) is valid because when solutions are computed with this local conservation condition, they differ very little from those obtained when a separate differential equation is employed for $Ca^i(x,t)$. Physically this means that the internal compartment does not notice the diffusion of calcium in the extracellular space, only the local fluxes through the membrane.

There are a number of properties of the model to be addressed. These concern the wave shapes, amplitudes, speeds and special phenomena such as subthreshold responses, multiple waves in response to a sustained stimulus and collision of SD waves. It was found that the wave shape is primarily determined by the pump strengths relative to the source term for potassium and the sink term for calcium. Though other quantities have some effect, the first subsection will be concerned only with the effects of changing k_2 and k_5.

Wave Shapes

SD is a solitary wave phenomenon though in practice spatial inhomogeneities in the cortical structure will alter the shape and speed as the wave propagates. The model equations predict some quite distinct wave shapes which have also been observed experimentally. In these results the following parameter and constant values were employed: $D_K = 2.5\times10^{-5}$ cm^2/sec., $D_{Ca} = 1.25\times10^{-5}$ cm^2/sec (though in the actual numerical computations these were set at scaled values of 2.5×10^{-3} and 1.25×10^{-3} which has no effect on the wave shapes: the other parameters are their actual values in the calculations with these scaled diffusion coefficients); the value of $RT/F \ln(\cdot)$ was set at $58\log_{10}(\cdot)$ which is appropriate at about 25°C; the resting external potassium and calcium ion concentrations were 2 mM and 1 mM respectively, the corresponding internal concentrations being 140 mM and 0.05 mM. The quantity $p_{Na}Na^o + p_{Cl}Cl^i$ was set at 9 mM and $p_{Na}Na^i + p_{Cl}Cl^o$ was set at 40 mM these being reasonable values based on Brinley (1963). The pump saturation rate parameters k_3 and k_6 are set at 10 and 40 which ensured maximal pumping with disturbances in the ion concentrations to levels where SD becomes possible. The values of α/β and α/γ were both set at 0.25 in these runs (Blinkov & Glezer, 1968), the effect of having different β and γ being discussed later. Since $K_R^o = 2$ mM the value of K_*^o was set at 2.2 mM. The value of k_7 was 0.11 and that of V_T set at 45 (based on the above experimental references).

With the source strength for potassium at $k_1 = 3$, the sink strength for calcium at $k_4 = 0.3$, the overall pump strength for potassium $k_2 = 208$ and the overall pump strength for calcium $k_5 = 2.08$, well formed solitary waves were formed as previously found (Tuckwell & Miura, 1978) in response to an initial condition of elevated K^+ (representing application of KCl) at the center of the unit interval (0, 1),

$$K^o(x,0) = 2+8\exp\{-[(x-0.5)/0.025]^2\}, \quad (18)$$

and an initial state of resting level calcium ion concentration

$$Ca^o(x,0) = 1. \quad (19)$$

Note that the initial level of external potassium is appreciably above resting level only on about 0.06 of the entire space interval. The spatial profiles of the stable solitary wave of increased external K^+ and decreased external Ca^{++} are shown in Figure 1A. The potassium rises to about 18 mM and the calcium falls to a very low level, about 0.02 mM. The return to resting level is accomplished quite rapidly for K^+ and somewhat more slowly for Ca^{++}.

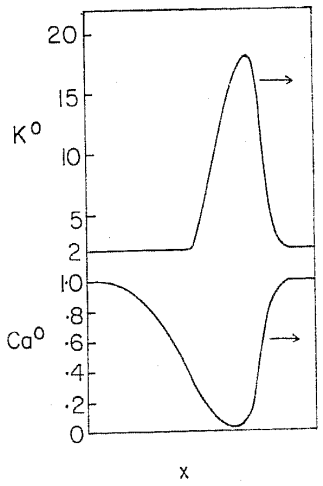

FIGURE 1A Solitary waves of elevated external potassium concentration, K°, and depressed external calcium concentration, Ca°, plotted against distance at fixed time. The units of K° and Ca° are mM/liter. These solutions are obtained by numerical integration of the model equations.

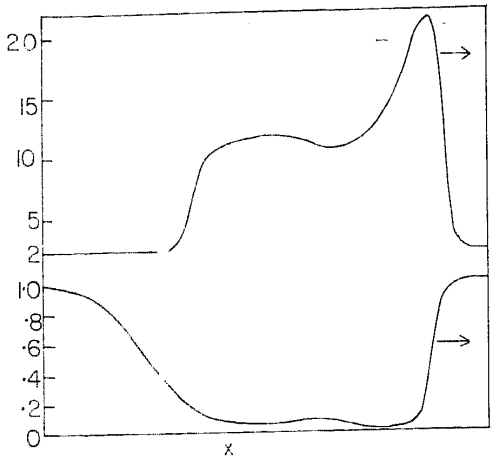

FIGURE 1B The wave profiles in space when the potassium pump strength is reduced. The tail of the K°-wave now has a secondary peak, as the wave orbit looped around the critical point (see Figure 2B).

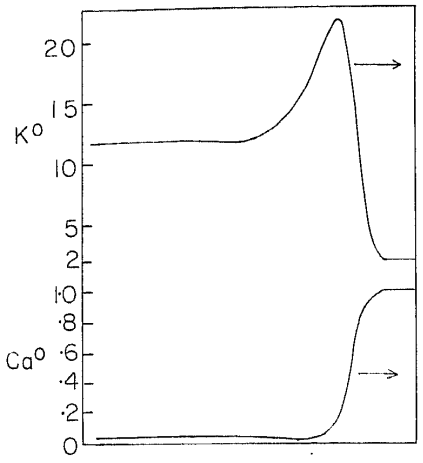

FIGURE 1C When the potassium pump is reduced in strength further, the tail of the wave does not go to resting level as the wave orbit goes straight to the critical point (see Figure 2C).

The various wave shapes can be obtained by changing the overall potassium pump strength k_2. If we increase k_2 to 249.6 (a factor of 1.2) then no wave forms at all. The K^+ level does rise above that applied and the Ca^{++} drops but there is a rapid return to resting levels. This is a subthreshold response. (Note, however, that there are some combinations of parameters whereby a wave will not propagate no matter how strong the applied stimulus.)

If we decrease the potassium pump strength slightly, the tail of the wave becomes longer representing more difficulty in returning to resting conditions. Eventually a different wave shape arises. Figure 1B indicates the profiles in space of the waves which form when the K-pump rate is decreased to 179. Now after the initial increase in K^+ and decrease in Ca^{++} there is an abortive attempt to return to resting levels. The latter are not achieved and the K^+ undergoes another slight increase whilst the Ca^{++} undergoes another slight decrease. This is followed by another attempt to return to resting level which is successful. We may say somewhat metaphorically that "the pump has won." The K^+ wave formed has a high sharp peak followed by a broader smaller peak. It is precisely this kind of response in measured K^+ concentration that was found in one case of SD in cat cortex by Sugaya *et al.* (1975, p. 831). Here the K^+ concentration rose to about 50 mM, fell to about 25, rose slightly and then fell back towards the original level. (Note that no TTX was applied.) On other occasions in that experiment and other experiments (Nicholson *et al.*, 1977) the K^+-wave has the appearance of that in Figure 1A.

A fourth kind of response is obtained with a weaker K-pump. The profiles of K^+ and Ca^{++} when the K-pump strength is reduced further to 166 are shown in Figure 1C. After the initial rise in K^+ there is a fall but only to about 12 mM whilst the calcium remains depressed at about 0.04 mM. It is difficult to say what the eventual level of the ion concentrations will be because the time to compute the solutions of the equations would be excessive. Either the levels remain at 12 and 0.04 indefinitely or there is an exceedingly slow return to lower levels (and possibly a final relatively rapid return to resting levels as in Figure 1B).

A fifth kind of response is possible. If the K-pump were effectively zero (and the Ca-pump) a saturating wave of about 23 mM for K^+ and 0.03 mM for Ca^{++} forms with no attempt to return to resting levels. This would correspond to "anoxic depolarization" where the level of K^+ rises to very high levels and remains there. In one study (Vyskocil *et al.*, 1972) the K^+ concentration rose to 100 mM whereas in SD the peak of the wave was about 65 mM at a depth of 0.5 mm. (Incidentally, the anoxic depolarization result can be used to estimate the resting internal concentration of K^+ (in this case for rat cortex) on the assumption that the final state has equal external and internal concentrations. If we assume the extracellular to intracellular volume ratio is 4:1, then we obtain

$K_R^i \simeq 125$ mM, which is consistent with other preparations (Brinley, 1963), but somewhat less than the value employed in these calculations).

The effects of changing the calcium pump strength were investigated but not so extensively. When the value of k_5 was increased to 2.29 stable solitary waves still formed of the same shape as in Figure 1A but the K^+ wave had a slightly (1 mM) larger amplitude. Also, when the Ca-pump was decreased to 1.66 a stable solitary wave again formed with slightly (1 mM) decreased amplitude of the K^+ peak.

These various kinds of response are made comprehensible when we consider the phase plane representations of the strengths of the reaction terms and the wave orbits. This is one of the distinct advantages of having just a two-component system. The idea is to plot the values of F amd G at various parts of the K^o–Ca^o plane to ascertain where they are positive and where they are negative. This has been done for the simplified model equations for SD (Tuckwell, 1979).

The most important feature of this analysis is the location of the "null isoclines" which are the curves in the K^o–Ca^o plane where $F = 0$ or $G = 0$. The intersection of the curves where $F = 0$ and $G = 0$ give equilibria or critical points for the corresponding system of ordinary differential equations. (That is, the equations obtained from (7) and (9) when $D_K = D_{Ca} = 0$). When this is done for the parameter values which gave rise to the waves of Figure 1A we obtain the null isoclines marked in Figure 2A. There are two curves where $F = 0$, the lower one corresponding to the rest state. The upper curve where $F = 0$ intersects the $G = 0$ curve in two places. The intersection to the right is an unstable equilibrium point and the one marked C is a stable spiral point. The position of C is the most important factor in determining the amplitude of the waves.

As the solitary wave passes a given point in space the values of K^o and Ca^o at that point move from the rest point R upward along the curve marked S (with arrows) and continue in an orbit around the critical point C to eventually return to R along $K^o = 2$. This is called the solitary wave trajectory. Note too that there are sinks for K^+ at $Ca^o = 1$ and $K^o < 6.3$ which implies that the system does have a threshold because if $K^o < 6$ and $Ca^o = 1$ there are no sources for K^+.

In Figure 2B the wave orbit is drawn for the parameter values that give the response indicated in Figure 1B. The null isoclines are omitted because they mask the wave trajectory but the critical point C is marked on the Figure. The $G = 0$ isocline is the same as in Figure 2A, the upper $F = 0$ isocline is somewhat lower. The orbit takes off from R, goes upward, and drops towards C. It loops around C once and then escapes from this attractor eventually to get back to the rest point R. This shows clearly that C is in fact a spiral point.

When the K-pump is decreased further, the upper $F = 0$ isocline shifts further downward and the critical point C is as shown in Figure 2C. The orbit of (K^o, Ca^o) values for the response of Figure 1C indicates a takeoff from R as before but

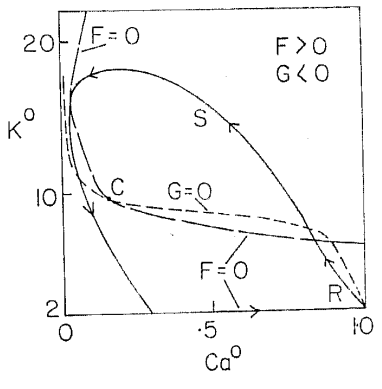

FIGURE 2A Phase portrait of K° and Ca°. The null isoclines for the system are shown by dashed lines. The upper critical point is marked C. Pairs of values of K° and Ca° that occur on the solitary wave of Figure 1A are plotted to give the solitary wave trajectory marked S which commences and ends at the rest point R. The arrows represent increasing time at a fixed space point.

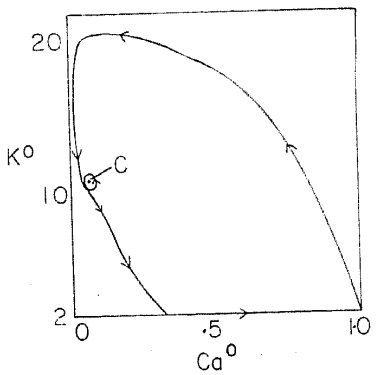

FIGURE 2B Phase portrait for the wave shown in Figure 1B, with null isoclines omitted to avoid overcrowding. The wave orbit this time loops around the upper critical point to give rise to the secondary peak in the wave tail, then returns to rest.

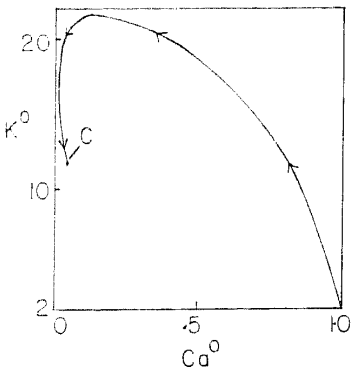

FIGURE 2C Phase portrait for the wave of Figure 1C. Here the wave orbit heads straight for the critical point and no return to rest state is apparent.

a decline which heads straight for C. This time the orbit seems to get stuck at C and a return to resting levels does not occur, at least in a reasonable time.

When the K-pump strength was increased the upper $F = 0$ curve is shifted so far upward that the initial stimulus of Eq. (18) does not give rise to a sufficiently large number of strong K^+ sources for the response to grow and spread. Anoxic depolarization would correspond to an initial point C high and to the left in the K^o–Ca^o plane and an orbit which goes straight to the critical point with no decline in K^o or increase in Ca^o.

Wave Speed and Amplitude

The position of the critical point C is important in determining wave amplitudes because the solitary wave orbit must go around C and, as seen above, clear it by a good margin in order not to get drawn into C. For a given location of C, waves of various amplitudes are possible and it has been found that the take off from R is the important factor in determining the solitary wave orbit. The question arises as to the factors which determine the wave speed. One of the neceesary tests of a model of SD is that it be capable of predicting waves with not only the correct amplitudes and shapes but also the correct velocity.

With the same values of the parameters and constants as in the last subsection various values of the potassium and calcium pump strengths were employed. The response of the system to the initial data of Eqs. (18) and (19) was ascertained numerically. In particular the type of response was noted (i.e., which of the responses depicted in Figures 1A, 1B, 1C or no wave at all), the value of the potassium concentration at the peak of the K^+-wave and the value of the calcium concentration at the minimum of the Ca^{++}-wave and the velocity of the waves as found from the computer print out of the solutions of the model equations. The results are given in Table I. In two cases no wave was obtained at all (K-pump too strong). In most cases well-formed solitary waves were obtained except in three cases where the response was as in either Figure 1B or 1C.

TABLE I

Properties of the solutions of the model equations for various values of the potassium (k_2) and calcium (k_5) pump strengths. The response type (column 3) is according to Figures 1A, 1B, 1C or no wave at all. The maximum external potassium concentration, K°_{max}, and the minimum external calcium concentration, Ca°_{min}, are given in columns 4 and 5. The fifth column contains the velocity of the wave relative to the velocity of the slowest wave obtained in this set of calculated solutions.

k_2	k_5	Response	K°_{max}	Ca°_{min}	V
208	2.08	1A	18.1	0.033	1.31
179	2.08	1B	20.8	0.017	1.95
185	2.08	1A	20.2	0.019	1.89
208	1.66	1A	16.6	0.052	1.00
250	2.08	No wave	—	—	—
166	2.08	1C	21.5	0.016	2.21
187	2.08	1A	20.1	0.019	1.77
177	2.08	1B	20.9	0.017	2.11
208	2.29	1A	18.6	0.031	1.38
181	2.08	1A	20.6	0.018	1.94
229	2.08	No wave	—	—	—
183	2.08	1A	20.5	0.018	1.89
208	2.50	1A	19.0	0.029	1.42
208	1.87	1A	17.5	0.040	1.22
179	1.66	1A	20.3	0.016	1.94

A variety of amplitudes of the K^+-waves and Ca^{++}-waves is observed. The greatest K^+ amplitude obtained is 21.5 mM with corresponding Ca^{++} amplitude 0.016 mM, this being a wave as in Figure 1C. The smallest K^+ amplitude obtained is 16.6 mM with corresponding Ca^{++} amplitude of 0.052 mM.

One notices the correlation between the amplitudes of the K^+-wave and the Ca^{++}-wave. These are plotted against each other in Figure 3A. The points do not lie on a smooth curve because there is a slight inaccuracy in estimating maxima and minima from the computer print out which is only at discrete space points. It is clear, however, that there is an inverse relation between the K^+-maximum and the Ca^{++}-minimum. This is simply a

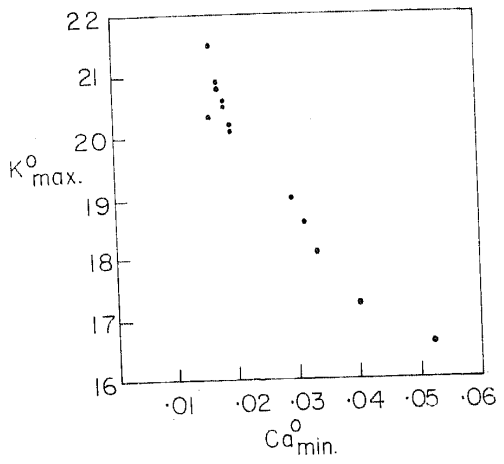

FIGURE 3A A plot of the peak value of K° versus the minimum value of Ca° for the various waves obtained when the pump strengths are varied as in Table I.

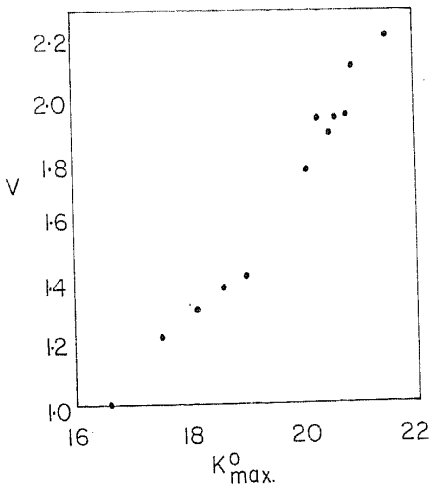

FIGURE 3B A plot of wave speed versus peak value of K° for the waves tabulated in Table I.

consequence of the fact that when the orbit goes higher in the (K^o, Ca^o) plane it spends more "time" in the region where $G<0$ and so swings further to the left, making the Ca^{++}-minimum smaller.

The amplitude of the wave seems to be the major factor in determining the wave speed. The velocity of the waves in the model system is plotted against the K^+-maximum in Figure 3B. The smallest velocity was for a wave with the smallest K^+-maximum (16.6 mM) and this is taken as the standard velocity of 1.00. The velocity of each of the remaining waves was computed relative to this standard. The velocity versus amplitude of the K^+-wave is plotted in Figure 3B. This is most revealing as it can be seen that in the range investigated the velocity is closely proportional to the amplitude of the K^+-wave. If one draws a (visual) best fit straight line through these points one obtains the relation, velocity $= 0.243 \times K^+$-maximum $-$ 3.05. If one then extrapolates back to $V = 0$ one obtains a corresponding K^+-maximum of 12.7. This makes good sense because this is the approximate value of K^o at the critical point C and clearly the K^+-maximum must be greater than this because the solitary wave orbit has to go around C. More will be said about velocity versus amplitude later when a comparison with experiment is made.

Effects of Remaining Parameters

In the simplified system of equations for K^o and Ca^o there are twenty variable parameters and constants, including the temperature. Most of these have been varied to ascertain their effects on the propagation of the waves. In many cases the changes made had a dramatic effect and no wave formed at all. In all cases the explanation for the effects of the changes was sought in terms of what they did to the null isoclines in the K^o–Ca^o plane.

When the external resting potassium ion concentration was changed to 3 mM from 2 mM with all other parameters and constants the same, the essential properties of the solutions were unaltered, except the amplitude of the K^+-wave was now 19.7 mM as opposed to 18.2 mM with $K_R{}^o = 2$. With $K_R{}^o = 2$ and the internal resting level of Ca^{++} changed from 0.05 mM to 0.01 mM, solitary waves again formed but this time the amplitude of the K^+-wave was 19.4 mM. With $K_R{}^o = 2$ mM and $Ca_R{}^i = 0.05$ mM and the ratio of $\alpha/\beta(=\alpha/\gamma)$ changed from 0.25 to 0.1, solitary waves still formed of similar shape and speed, the K^+-amplitude being 18.7 mM. Hence the solutions are fairly insensitive to changes in the parameters $K_R{}^o$, $Ca_R{}^i$ and the ratio of the extracellular to intracellular space (assuming no distinction for this ratio in the cases of pre- and postsynaptic membrane). When both $K_R{}^o$ and $Ca_R{}^i$ were changed to the values 3 mM and 0.001 mM, solitary waves formed of amplitude 21.2 mM for K^o. The effects of the remaining parameter changes will be relative to this run.

The parameter V_T is the absolute value of the membrane potential at which the presynaptic calcium conductance attains its half maximal value.

In the results reported above this was set at +45 mV, based on available data. The solutions are quite sensitive to changes in V_T. When $V_T = 48$ the upper $F = 0$ isocline shifts far downwards and the system loses its threshold property. A wave might propagate but the Ca^o level would become so small that numerical computation is very difficult because the critical point C is now at about $K^o = 9$ and $Ca^o = 0.005$. (It should be pointed out that one of the difficulties in obtaining numerical solutions was that if the time step was too large and the Ca^o became very small, then the numerical scheme would predict a slightly negative value of Ca^o which would abort the computer run because the value of V_{Ca} would now involve the logarithm of a negative number.) When V_T was changed to 42, the $F = 0$ and $G = 0$ isoclines were both shifted upward in the K^o–Ca^o plane and there was no propagating event in response to locally elevated K^o.

The remaining parameter which is contained in the presynaptic calcium conductance function $g(V)$ is k_7. This determines the slope of the rise of calcium conductance with depolarization. The standard value based on available data is $k_7 = 0.11$. The solutions are also very sensitive to changes in this parameter. When k_7 was changed to 0.08, a wave formed of the type depicted in Figure 1C. The amplitude of the K^+-wave was 24.2 mM and the tail came back to 9.9 mM, the corresponding values of the external calcium concentration being 0.01 mM and 0.02 mM. This wave travelled considerably faster (about 4.5 times) than the similar response with $k_7 = 0.11$, but this is probably due to the fact that the upper $F = 0$ isocline is almost coincident with the one at the resting level of K^o so that there is no threshold for production of potassium. When k_7 was changed to 0.14 there was no propagating event though an increase in K^o and decrease in Ca^o did occur immediately after the application of the additional K^+. A small wave of K^+ did form but it quickly died out. The upper $F = 0$ isocline is here shifted upward in the K^o–Ca^o plane making far fewer sources of K^+ at low levels of this ion.

We now consider the effects of changing the pump saturation rate parameters. Recall that previously the K^+-pump saturation rate parameter was $k_3 = 10$. When k_3 was changed to 7.5 a solitary wave still formed with an amplitude for K^o of 21.4 mM compared with the previous amplitude of 21.2 mM. The solutions are thus somewhat insensitive to changes in this parameter. This can be explained readily by the fact that the null isoclines are hardly shifted except for values of K^o near resting level because there the K^+-pump has not achieved its maximal value.

The effects of varying the calcium pump saturation rate parameter, k_6, were also not very great. Recall that previously $k_6 = 40$. When this parameter was changed to 50, the solitary wave formed with the same amplitude for K^o of 21.2 mM. When k_6 was changed to 30, the wave amplitude was hardly altered, being now 21.2 mM. The explanation for the insensitivity pf the solutions to these large changes in k_6 is immediate in terms of their minor effect on the null isoclines of F and G.

The resting concentrations of the other ions, Na^+ and Cl^- can also be varied. Previously we had $p_{Na}Na^o + p_{Cl}Cl^i = 9$ mM. The effect of increasing this quantity can be considered as either due to increased external sodium concentration or increased internal chloride concentration. When the value 20 mM was employed rather than 9 mM the upper $F = 0$ and the $G = 0$ isocline ran almost along the line $K^o = K_R{}^o$. The system therefore had no threshold and the K^o level rose quickly to over 50 mM and the Ca^o level fell to about 0.02 mM. Thus increased external sodium or increased internal chloride have a facilitating influence, probably because they both lead to a more depolarized (equilibrium) state of the membrane. As expected therefore when $p_{Na}Na^o + p_{Cl}Cl^i$ was decreased an antagonistic effect was produced and no wave emerged from the stimulus. In fact the K^o level declined everywhere where it was above resting level and the Ca^o level hardly changed from its resting level. Here the upper $F = 0$ isocline was shifted to very large values of K^o and the $G = 0$ isocline was also shifted upward in the K^o–Ca^o-plane.

The quantity $p_{Na}Na^i + p_{Cl}Cl^i$ had previously been set at 40 mM. When this was changed to 30 mM the upper $F = 0$ isocline was shifted downward in the K^o–Ca^o plane and so was the $G = 0$ isocline to a lesser extent. The critical point C occurs at such a small value of Ca^o that a numerical solution of the system becomes very difficult. When the value of $p_{Na}Na^i + p_{Cl}Cl^i$ was increased to 50 mM the upper $F = 0$ isocline attained a new aspect. The curve now bent over at higher K^o values from the left part of $K^o - Ca^o$ plane and went towards the $Ca^o = Ca_0{}^R$ line. Thus there are now sinks for K^+ at small and high levels of K^o and this is readily explainable as being due to the fact that $(V - V_K)$ changes sign at high

K^o values. The threshold was now much higher also and the same stimulus which had previously given rise to stable propagating waves now gave rise to a nonpropagating event. This change can be construed as an increase in external chloride concentration and this according to the model is an antagonistic effect. This is supported by experimental evidence (Bures *et al.*, 1974) because raising the extracellular levels of chloride ions leads to a "chloride block" of SD.

The resting level of internal K^+ concentration has heretofore been set at 140 mM. When this was increased to 155 mM there was no solitary wave in response to the initial data of Eqs. (18) and (19). This is readily explainable as being due to the hyperpolarizing effect of the increased internal K^+ concentration. The critical point C was now at (10, 0.3) so a wave would probably exist if the other constants were varied. When the resting internal K^+ concentration was decreased to 125 mM, the upper $F = 0$ isocline was shifted downwards and the point C was now at about (9, 0.02). A wave may form under these conditions but its numerical computation is difficult.

Threshold and Multiple Waves

When a suprathreshold concentration of KCl is applied to the cortical surface a train of SD waves issues forth (see, for example, Mayevsky & Chance, 1974). How the larger concentrations of K^+ should be incorporated into the model equations is difficult to assess. The reason for this is that the KCl solution applied may seep through the dura and it is not known how rapidly this occurs. There is also the possibility that cells in the immediate neighbourhood of the strong applied stimulus lose their viability. It was decided to maintain a stimulus to represent very large concentrations of applied KCl. This was done for a region in space corresponding to about 1 mm of cortical surface. Thus, the model equations are now integrated with the constraint

$$K^o(x, t) = K_A,\ x_1 \leqslant x \leqslant x_2,\ t > 0, \qquad (20)$$

K_A representing the strength of the sustained stimulus. With the system being solved on the unit interval, the values $x_1 = 0.175$ and $x_2 = 0.225$ were employed. The parameters and constants were set at the values that had previously given rise to the wave shown in Figure 1A, with a resting level of external potassium of 2 mM. With an applied stimulus of $K_A = 8$ mM, no waves emerged. This was also the case when K_A was set at 10 mM. When, however, K_A was raised to 12 mM a wave appeared, somewhat hesitantly. Thus, the threshold concentration of K^+ for eliciting an SD wave was between 10 and 12 mM for the model system. This value compares favourably with the value of just above 10 mM reported experimentally by Kraig and Nicholson (1978). When the strength of the sustained stimulus was increased to $K_A = 21$ mM a train of SD waves issued forth. The distribution of external K^+ when two such waves had formed is shown in Figure 4. These waves are practically identical. As the strength of the stimulus is increased the time between successive waves becomes smaller in both theory (as shown in the simplified model system, Tuckwell, Ref. Note 1) and in experimentally induced SD in rat cortex (Mayevsky & Chance, 1974).

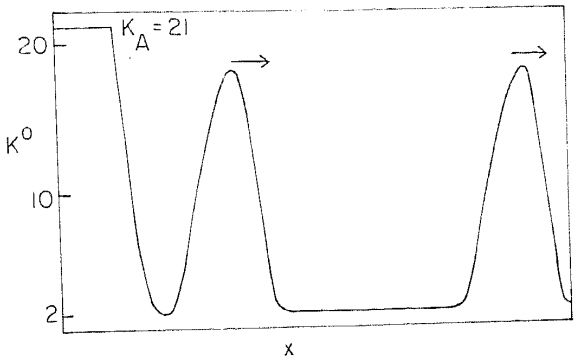

FIGURE 4 Multiple waves issuing forth from a sustained stimulus of elevated external K^+ concentration.

Comparison of Theory with Experimental Results on TTX-Treated Cortex

It is apparent that the wave amplitude for both K^+ and Ca^{++} depends upon the position of the critical point C. The position of this critical point may be shifted around by varying the constants and parameters of the model equations. It was decided to ascertain whether the wave form reported for K^+ in TTX-treated cat cerebral cortex (Sugaya *et al.*, 1975) could be closely approximated by solutions of the model equations for certain values of the constants and parameters. Matching the time variation of the K^+ concentration in experiment and theory enables the correct time scale in the equations to be established so that the velocity of propagation can be then computed.

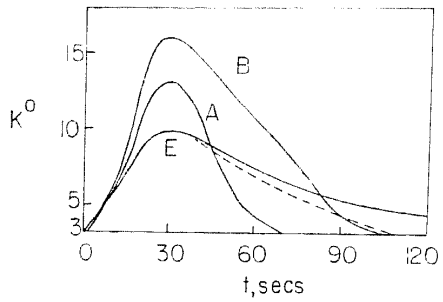

FIGURE 5 Low amplitude K^+-waves for the model without action potentials plotted at fixed x as a function of time. The experimental result of Sugaya *et al.* (1975) is marked E which is possibly not the maximum amplitude. The smallest wave obtained in the model system is marked A which has K^+ returning to rest somewhat rapidly. When the return to rest is made a little slower (B) the amplitude of the calculated response grows. The dashed line is the experimental result adjusted so that the end result is resting K^+ concentration.

Numerous attempts were made in this direction but it proved quite difficult to obtain what could be called an excellent match of theoretical and known experimental results in this case. In Figure 5 are shown the experimental results for K^+ concentration in cat neocortex treated with TTX and two sets of results obtained from the model equations. The lower theoretical result (marked A) has the smallest amplitude for the K^+-wave that was achieved in many attempts. This K^+-wave has an amplitude of 13.3 mM with a resting level of 3 mM, whereas the experimental result has an amplitude of 10 mM and the same resting level. In the Figure the time scale of the predicted K^+ variation has been adjusted so that the peaks of the theoretical and experimental curves pccur at about the same time. The calcium ion concentration was not measured in this experiment and the predicted Ca^o level falls from its resting level of 1 mM to 0.24 mM. With diffusion coefficients scaled to "D_K" = 0.0024 and "D_{Ca}" = 0.001, the values of the constants which gave this smallest theoretical amplitude for the K^+-wave were: $\alpha/\beta = \alpha/\gamma = 0.25$, $k_1 = 1.882$, $k_2 = 88.07$, $k_3 = 2.5$, $k_4 = 0.230$, $k_5 = 1.318$, $k_6 = 44.44$, $K_R{}^o = 3$ mM, $Ca_R{}^o = 1$ mM, $Ca_R{}^i = 0.001$ mM, $K_R{}^i = 140$ mM, $RT/F\ln(\cdot) = 58\log_{10}(\cdot)$, $p_{Na}Na^o + p_{Cl}Cl^i = 9$ mM, $p_{Na}Na^i + p_{Cl}Cl^o = 55$ mM, $k_7 = 0.11$, $V_T = 45$ mV and $K_*{}^o = 3.2$ mM.

It can be seen that even though the amplitudes of the K^+ responses are close (13.3 mM versus 10 mM) the predicted K^+-concentration returns too rapidly to resting values. It is somewhat strange that the experimentally measured K^+ concentration appears not to return to resting value throughout the whole duration of the recording, unless the scale has become distorted and the horizontal (time) axis should be rotated a few degrees clockwise. This would give the time course of K^+ indicated by the dashed line in Figure 5.

Given that the experimental and theoretical amplitudes of the K^+ waves are about the same, it is natural to try to make the tail of the theoretical wave come down more slowly to get better agreement. Unfortunately, perhaps, when this is attempted, the amplitude of the predicted result grows. Such a set of results is depicted by the curve marked B in Figure 5. The parameters and constants for this run are as in the result A except now the potassium pump strength is reduced by a factor of 0.85 to $k_2 = 74.86$. Now the predicted amplitude of the K^+-wave is 16.7 mM even though the time course is in better agreement with experimental result, especially the dashed line in Figure 5.

There is another aspect of the above comparisons. It is not known what the maximum K^+ concentration amplitude is in the experimental situation because the amplitude has been shown to depend on the depth at which the recording is made (Vyskocil *et al.*, 1972, for example). In the results with TTX treated cortex a recording was made at a single depth only. Consequently, the true amplitude of the wave (which is by definition the maximum amplitude) may be somewhat higher than the apparent 10 mM amplitude reported by Sugaya *et al.* (1975).

Once the times from resting state to peak value of K^+ concentration are made approximately the same in the theoretical and experimental results one can calculate the velocity of propagation of the waves in the model system. The way this is done is as follows. Suppose the original equation for the evolution of the K^+ concentration in the actual brain structure is

$$\frac{\partial K^o}{\partial t} = D_K \frac{\partial^2 K^o}{\partial x^2} + F(\mathbf{C}) \qquad (21)$$

where $D_K = 2.4\times10^{-5}$ cm^2/sec, with x in units of cm and t in secs. The numerical results were obtained with "D_K" $= 2.4\times10^{-3}$ to make the wave propagate at a reasonable rate on the unit interval. Suppose we have set $X = ax$ and $T = bt$. Then Eq. (21) becomes

$$\frac{\partial K^o}{\partial T} = \frac{D_K a^2}{b}\frac{\partial^2 K^o}{\partial x^2} + \frac{F(C)}{b}$$

$$= \text{“}D_K\text{”}\frac{\partial^2 K^o}{\partial x^2} + \frac{F(C)}{b} \qquad (22)$$

Once the time courses of the experimental and theoretical results are matched, the time scaling factor b is determined. Then, since “D_K” = $D_K a^2/b$ and “D_K” was set at 2.4×10^{-3} in the numerical calculations, we have a fixed distance scaling factor a. The velocity of the waves in the numerical results, $\Delta X/\Delta T$, can then be converted to the velocity $v = \Delta x/\Delta t$ in the brain structure because $\Delta x/\Delta t = (b/a)\ \Delta X/\Delta T$.

When these velocity calculations are done for the result marked A in Figure 5, the velocity is $v = 0.65$ mm/min. This should be divided by $\pi/2$ to allow for the fact that x in the cortex is stretched out because the path of the ions is made tortuous by (assumed cylindrical) obstacles consisting of the various cell processes. This is a great oversimplification but it will suffice here. The predicted velocity then becomes 0.41 mm/minute. The wave with the slightly larger amplitude and longer overall time course (B) has a corresponding velocity of 0.83 mm/min.

The accepted mean experimental velocity of SD in mammalian neocortex is about 3 mm/min (Bures *et al.*, 1974) but this is the value for normal cortex, untreated with TTX. From the results of Sugaya *et al.* (1975, p. 825, Figure 3) their measured velocity of SD in cat cortex is very close to 2 mm/min. These authors make the following statements concerning SD propagation in TTX treated cortex: “SD can be evoked in the TTX region by KCl application and can propagate from the TTX region into the normal cortex. ... The velocity of propagation is labile, sometimes slower and sometimes faster than normal.” The velocity predicted by the model equations according to the response B in Figure 5 is 0.83 mm/min. which is certainly less than the normal experimental velocity of 2 mm/min. We will see that this predicted value is very reasonable when we consider the effects of action potentials on SD propagation. We also note that in some cases of SD in TTX treated cortex the amplitude of the K^+-wave was small (18 of 24 experiments) whereas in others the amplitude was the same in TTX treated and normal cortex. This suggests that in some cases the TTX was ineffective in blocking action potentials and under these conditions the velocity would be the approximately normal figure of 2 mm/min.

Inclusion of Action Potentials

It is known that neurons undergo rapid spiking at the onset and recovery phases of SD in cortex untreated with TTX. It is also known that K^+ is released from nerve cells during spiking activity whilst at the same time there is an influx of Na^+. When a neuron fires rapidly it is expected to extrude K^+ by virtue of its own membrane permeability to K^+. It will, in a cortical structure rich with synaptic connections, also lead to further K^+ efflux by a sequence of events. When a neuron fires rapidly, we expect its terminals (many of which are intracortical) to undergo large and rapid depolarizations (much greater than due to the effect of increasing external K^+ because now the membrane potential at the terminal swings towards the sodium equilibrium potential) causing inward calcium currents which will release transmitter substances. The latter will lead to postsynaptic conductance changes and these, amongst other things, will cause additional efflux of K^+. Thus K^+ efflux occurs due to the primary event (action potential) and the secondary event (synaptic activation and transmission).

To incorporate action potentials in a model for SD in a precise way is not feasible. Each nerve cell would have to be represented by its own Hodgkin–Huxley type patch of membrane and when we smooth out cell boundaries we would have a continuum of nerve cells and hence the Hodgkin–Huxley equations would need to be parametrized by the space variable x. In addition, at each space point we would need to consider an additional variable, V^* (x, t), which is the instantaneous membrane potential driving the capacitative currents across the cell membrane. A further complication which would make numerical computation exceedingly difficult is that the time scale for voltage fluctuations during action potentials is in the order of milliseconds, whereas the natural time scale for SD is in seconds. All these complications make an approximate, rather than exact, inclusion of the effects of action potentials during SD a worthwhile undertaking. The test of the usefulness of an approximate treatment can only be how well it makes correct qualitative and quantitative predictions concerning the ion fluxes during SD.

To illustrate how the approximation to be employed arises, consider the qualitative behavior

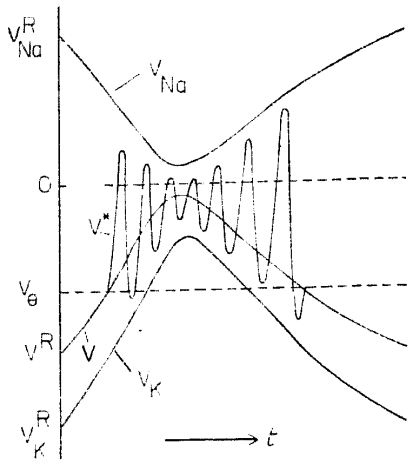

FIGURE 6 Expected time courses of the various potentials at a fixed space point as the SD wave passes. V_{Na} and V_K are the sodium and potassium equilibrium potentials which commence and end at their resting values $V_{Na}{}^R$ and $V_K{}^R$. The equilibrium membrane potential is V and V^* is the instantaneous membrane potential. When V gets to V_θ, the threshold for action potentials, V^* oscillates between near V_{Na} and near V_K.

of the various potentials during SD when action potentials are present. In Figure 6 is shown schematically how the quantities V_K, V_{Na} and V, the various equilibrium potentials, and V^*, the instantaneous membrane potential, will change during SD. These behaviors are based on ion concentration measurements and observations of neuronal spiking during SD (Goldensohn & Walsh, 1968; Kraig & Nicholson, 1978). Also marked on the figure is a threshold potential, V_θ, for action potential generation. When this is attained by V spiking occurs rapidly (each "spike" in the Figure represents several, possibly up to hundreds, of spikes). Each time a spike occurs the instantaneous membrane potential V^* swings upward to the vicinity of the sodium equilibrium potential V_{Na}, then swings downward to the vicinity of the potassium equilibrium potential, V_K. According to the Hodgkin–Huxley theory, the ion fluxes during such events are, for potassium for example, $g_K(V^*)(V^*-V_K)$ where $g_K(V^*)$ is the membrane conductance to K^+ at the voltage V^*. Furthermore, the frequency ϕ of action potentials depends on the relative positions of the equilibrium potentials, or equivalently, the concentrations of the ions. Hence if $\phi(\mathbf{C})$ is in spikes per second, with $\mathbf{C}$ fixed, the rate of change of external K^+ concentration is,

$$f(\mathbf{C}) = c_1\phi(\mathbf{C})\int_0^{\Delta T} g_K(V^*-V_K)dt', \qquad (23)$$

where ΔT is the duration of one spike, c_1 is a constant, V^* is the potential as a solution of the Hodgkin-Huxley (1952) equations, and t' is time elapsed since the beginning of a spike. Since we know that V^* swings from near V, the membrane equilibrium potential, to near V_{Na}, down to near V_K and back to V, the simplest procedure is to replace V^* by its approximate average value during a spike. This is called "time-coarsegraining" and is a procedure similar to that adopted by Wilson & Cowan (1973). As the average value of V^* we take the average of the sodium and potassium equilibrium potentials. Hence,

$$f(\mathbf{C}, V^*) \simeq f^*(\mathbf{C}) = c_1' g_K\left(\frac{V_{Na}+V_K}{2}\right) \times\left(\frac{V_{Na}+V_K}{2}-V_K\right)\phi(\mathbf{C}) \qquad (24)$$

The function $\phi(\cdot)$ is not known. To obtain its full dependence on the ion concentrations would take an extremely large number of computer generated solutions of the Hodgkin–Huxley equations. A reasonable estimate is therefore imperative. ϕ is decomposed into two factors one of which describes the input conductance, the other reflecting the frequency of firing at various membrane potentials. It is assumed that the cells have a threshold membrane potential V_θ so that when $V<V_\theta$, no action potentials are fired and hence $\phi = 0$. As V climbs above V_θ, ϕ must increase, but not without limit. When V gets to 0, representing a completely depolarized cell, ϕ must again be zero. Hence the

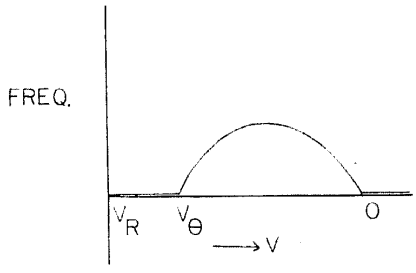

FIGURE 7 The assumed form of the dependence of the frequency of action potentials on equilibrium membrane potential V at fixed calcium concentration. The frequency is zero below the threshold V_θ for action potentials in the resting state, climbs to a maximum and declines to zero when the cell is completely depolarized.

simplest feasible assumption is that ϕ increases from 0 at $V = V_\theta$, achieves a maximum and then declines to 0 at $V = 0$. The behavior of ϕ as V varies (recall that V depends on C) is sketched in Figure 7. A suitable approximating function is a portion of a parabola that passes through $(V_\theta,0)$ and (0, 0). The frequency of firing must also depend on the calcium concentration, because if this were extremely low there would be less calcium influx into presynaptic terminals, less transmitter released, and hence less postsynaptic conductance, which is the input conductance to the cells. The simplest assumption is that the frequency of firing, at fixed, V, V_K and V_{Na} is proportional to the input conductance which is taken to be proportional to the effective transmitter concentration in the synaptic clefts. The latter is (Tuckwell & Miura, 1978) $\sim g(V)\ (V-V_{Ca})$. In the numerical calculations we assume that g_K does not vary much and can be taken as a constant. Hence the final form for source term for K^+ in this very approximate treatment is

$$f(\mathbf{C}) = -cV(V_0-V)[(V_{Na}+V_K)/2-V_K] \times (V-V_{Ca})\,g(V)\,H(V-V_\theta) \qquad (25)$$

where c is a constant.

Before proceeding with the introduction of this extra term into the potassium reaction term a point must be made about the calcium level. The level to which Ca^o drops is determined by the position of the critical point C. Furthermore if the Ca^o value drops too low, problems arise in the numerical integration of the reaction diffusion equations as pointed out above. It proved very difficult to get the critical point to shift to large values of Ca^o until it was realized that the ratio α/γ had a considerable influence. It was found that with $\alpha/\gamma = 1$ and $\alpha/\beta = 0.25$ (as before) a wave could be obtained with a K^+ maximum of about 17 mM and a Ca^{++} minimum as high as 0.4 mM, whereas previously when $\alpha/\beta = \alpha/\gamma = 0.25$ the calcium would usually drop to very small values. This change in α/γ comes about from the following reasoning. The presynaptic terminals can perhaps be considered to be localized little compartments as evidenced by the fact that synaptosomes themselves are quite viable (Campbell, 1976). Thus, the ratio of the extracellular volume to the effective intracellular volume may be much larger for presynaptic compartments than for postsynaptic compartments. This means that it will take less calcium loss from the extracellular space to cause the term $(V-V_C)$ to change sign and this will shift the null isocline for G to the right in the (K^o, Ca^o)-plane.

With this modification to the parameters the action potential term was now included in the model equations and the effects of varying the constant c in equation (25) ascertained. With $c = 0$ the following parameters were employed: "D_K" $= 2.4\times10^{-3}$, "D_{Ca}" $= 1.0\times10^{-3}$, $\alpha/\beta = 0.25$, $\alpha/\gamma = 1.$, $k_1 = 3.76$, $k_2 = 176$, $k_3 = 2.5$, $k_4 = 0.0826$, $k_5 = 0.474$, $k_6 = 10$, $K_R{}^o = 3$ mM, $Ca_R{}^o = 1$ mM, $Ca_R{}^i = 0.001$ mM, $K_R{}^i = 140$ mM, $RT/F \ln(\cdot) = 58 \log_{10}(\cdot)$, $p_{Na}Na^o + p_{Cl}Cl^i = 9$ mM, $p_{Na}Na^i + p_{Cl}Cl^o = 55$ mM, $k_7 = 0.11$, $V_T = 45$ mm and $K_*{}^o = 3.2$ mM. In response to the initial data of Eqs. (18) and (19), stable propagating waves of elevated K^+ and depressed Ca^{++} emerged from the stimulus, the maximum K^+ level being 16.8 mM and the minimum Ca^{++} level being 0.4 mM.

A typical threshold potential for action potentials is for CNS cells is about 10 or 12 mV above resting level (Calvin, 1975). Since the resting membrane potential with the above constants and parameters is $V_R = -70.2$ mV, the value of V_θ was taken to be -60 mV. The sodium equilibrium potential was set at 60 mV. Though this quantity will vary considerably when the movement of sodium ions with action potentials is taken into account the qualitative effects will be preserved.

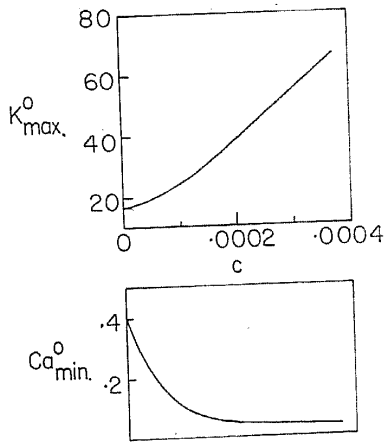

FIGURE 8 Peak value of the potassium wave plotted against the minimum value of the calcium wave as a function of the parameter c in the model which includes action potentials.

The wave obtained with $c = 0$ corresponds now to the case of SD in TTX treated cortex. When the value of c is made nonzero the amplitude of the wave obtained grows. The following values of c

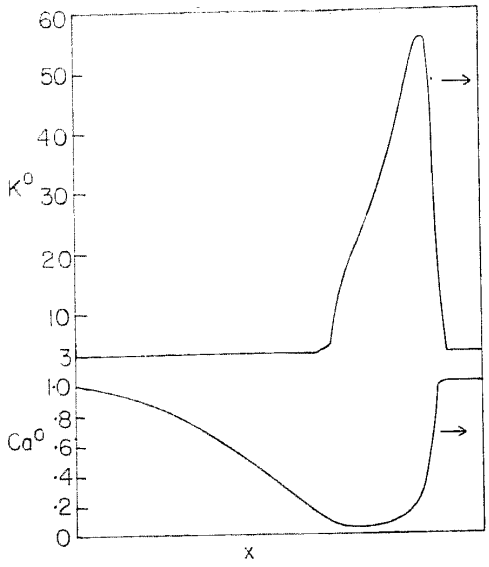

FIGURE 9A An example of the large amplitude K^+-waves obtained when action potentials are included in the model.

were tried: 0.0001, 0.0002, 0.00025, 0.0003 and 0.000375. The amplitude of the K^+-wave and the amplitude of the Ca^{++}-wave are plotted against c in Figure 8. After an initial slightly nonlinear increase, the peak value of the external potassium ion concentration, K^o_{max}, grows approximately linearly with c. The minimum value of the calcium ion concentration, Ca^o_{min}, has an initial slightly nonlinear decrease followed by a gentle decline as the value of c increases past 0.00015. A typical result is shown in Figure 9A where the profiles in space of the K^o- and Ca^o-waves are shown at a fixed time for $c = 0.0003$. The basic wave shape is similar to that without action potentials, the most remarkable difference being in the velocity of propagation. The phase portrait for this wave is shown in Figure 9B, there the K^+ and Ca^{++} reaction term null isoclines are indicated as well as the solitary wave trajectory S. The qualitative features of the phase portrait are unaltered, the upper critical point C being at about (10, 0.3).

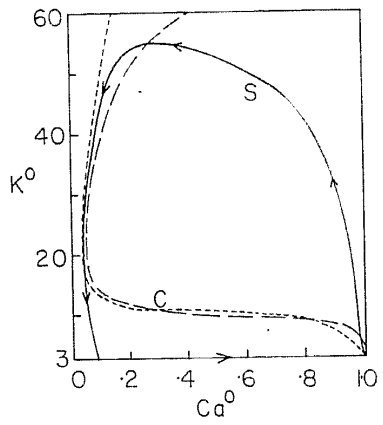

FIGURE 9B Phase portrait of the wave of Figure 9A. The dashed lines are the null isoclines of F and G, the solitary wave trajectory is marked S.

As the wave amplitude grows so does the speed of the waves, as was noted in a previous subsection, for small amplitudes. Here, however, we can look at the relationship between speed and amplitude of the K^+-wave over a large range of amplitudes. There is, of course, a minimum velocity because the minimum amplitude is determined by the position of the critical point C. In Figure 10 is plotted the velocity of propagation of the waves against amplitude. The units of velocity here are the distances X moved in time $T = 1$ where X and T are the scaled space and time variables used in the numerical calculations. The points on Figure 9 have associated error bars because it is not possible to obtain the velocity precisely from a numerical calculation, the accuracy of distance measurements being limited by the space grid used in the calculations. (This was $\Delta X = 0.01$ in all cases and the results in the model with action potentials are obtained with time step $\Delta T = 0.01$. If the calcium level drops very close to zero, a much smaller time

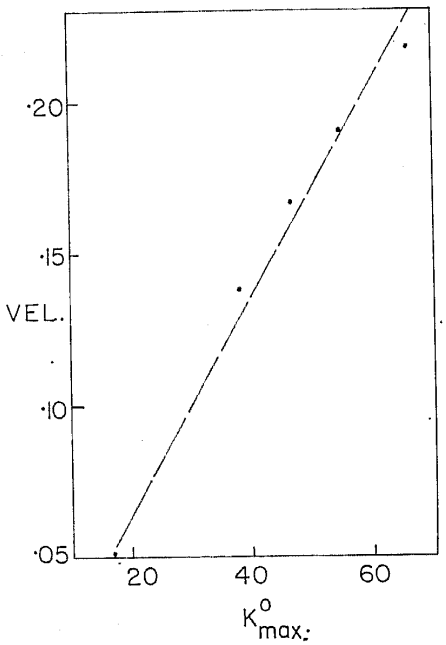

FIGURE 10 Velocity of the large amplitude waves versus the peak value of the K^+ concentration. The unit of the velocity is in scaled variables X and T. A linear relation is apparent.

step is necessary making numerical computation difficult.)

Comparison with Experiment

We can next examine a set of experimental data on the time course of K^o during SD in a normal brain structure and match both the amplitude the approximate time course as was done previously for TTX treated cortex.

The most detailed data are given for rat cortex by Vyskocil *et al.* (1972), in the sense that the amplitude and time course were reported at various depths. By definition, the amplitude of the wave is the maximum amplitude, (note that in the cortex, the solitary wave is not a curve but a surface), and the value reported in that study was 64.6+7.2 mM at a depth of 0.5 mm. For $c = 0.000375$ in the model equations with action potentials a wave of K^+-amplitude 66 mM was obtained. When the duration of the K^o increase in the above mentioned experiment and the theoretical wave of about the same amplitude are matched, the velocity of propagation of the theoretical waves is, after allowing for the tortuosity of the path, 2.9 mm/min., which compares favourably with the mean experimental velocity of 3 mm/min (Bures *et al.*, 1974).

For catfish cerebellum (Kraig & Nicholson, 1978) the distribution of amplitude of the K^+-wave with depth was not given. Using the available data and matching the experimental K^+-wave with a theoretical one of amplitude about 40 mM ($c = 0.0002$) gives a predicted velocity of 0.51 mm/min which is just inside the experimental range of 0.5–1.5 mm/min.

A comparison is also possible for cat neocortex, though again the amplitude distribution with depth is not given (Sugaya *et al.*, 1975). A K^+-wave of amplitude 55 mM ($c = 0.0003$) obtained in the theoretical results was matched for duration with the experimentally measured K^o level. In this case the velocity predicted by the model is 1.33 mm/min which is somewhat less than the experimental value of 2 mm/min. If the K^+-wave has a somewhat greater amplitude at a different depth then the predicted velocity would be closer to the experimental one.

A final comparison is made for the K^+-wave in cat cerebellum (Nicholson *et al.*, 1978). Again the variation in amplitude with depth is not known but the highest amplitude reported was about $K^o_{max} = 55$ mM. The predicted velocity in this case is 1.82 mm/min whereas the experimental report gives 9 mm/min. This is a large discrepancy for which there are two possible explanations. The first is that the experimental value is not correct. This is a possibility because the velocity of propagation was not measured directly but obtained by a comparison with an early measurement of the velocity of propagation of impulses in parallel fibers (Eccles *et al.*, 1966). The second possibility is that the model is inadequate. In the cases where reasonable agreement between experimental and predicted velocities of SD is obtained, it is likely that diffusion of ions alone is capable of accounting for the spread of the wave. Other factors not included in the model may contribute to the advance of the SD wave. Amongst these are electrotonic spread of depolarization along fibers running parallel to the cortical surface and the spatially extended excitation and inhibition of cells ahead of the wave by synaptic contacts which are known to extend up to several hundred microns. When the velocity of SD is measured directly in the cat cerebellum, which is the one preparation where the model and experimental velocities are in disagreement, we will be able to ascertain whether diffusion alone can explain the advance of the wave of spreading cortical depression. It is pointed out that the velocity comparisons made here will not be changed in detail very much when the fluxes of the other ions (Na^+, Cl^-) and neurotransmitter substances (e.g., glutamate, GABA) are included in the model because we have found that their inclusion does not strongly influence the velocity of propagation.

Finally, it was decided to investigate the effect of allowing for the decrease in internal potassium concentration during SD by letting $K^i(x, t)$ vary according to

$$K^i(x, t) = K_R{}^i - \frac{\alpha}{\beta}[K^o(x, t) - K_R{}^o], \qquad (26)$$

where subscripts R denote resting levels. With action potentials included and $c = 0.0003$ in Eq. (25) the K^o-wave now formed and propagated, its amplitude now being 49 mM in comparison with an amplitude of about 55 mM when the K^i level was held fixed at $K_R{}^i$. The amplitude of the Ca^o-wave was practically unaltered, and the velocity of propagation slightly less in accordance with the apparent linear relation between velocity and amplitude of the K^o-wave.

CONCLUSIONS

Spreading depression is a very complicated wave phenomenon which involves fluxes of K^+, Ca^{++}, Na^+, Cl^-, neurotransmitters and probably other substances through various kinds of neuronal and glial membrane, by an assortment of dynamical processes. The spread of SD may involve mainly diffusion or diffusion coupled with the synaptic activity induced ahead of the wave by neuronal firing and possibly also electrotonic spread of depolarization along fibers parallel to the cortical surface. An excellent discussion of possible mechanisms and processes involved in SD, many of which have not been mentioned in this article, can be found in Kraig and Nicholson (1978).

The ideas proposed previously (Tuckwell and Miura, 1978) and expanded upon here seem to contain the essence of a theory of SD. The model consists of a coupled system of nonlinear reaction-diffusion equations which have the capability of supporting solitary waves as occur in SD. The components of the system are the concentrations of the various ions and the effects of neurotransmitters are implicit in the equations. Here attention has been focused on the ions K^+ and Ca^{++} as these ions play important roles in SD, and one has the advantage of being able to reduce the system to a two component one which makes for an understanding of phase portraits and also computational efficiency. When the effects of action potentials are taken into account, in an albeit simplified way, the exact inclusion via the Hodgkin–Huxley equations not being feasible, the model makes the following predictions: (1) The existence of a threshold concentration of external K^+ concentration of around 10 mM for elicitation of an SD wave (2) Solitary waves of increased external K^+ concentration and diminished Ca^{++} concentration (3) The increase in the K^+ concentration occurs before the decrease in Ca^{++} concentration (4) The return to resting Ca^{++} levels occurs after the return of K^+ to its resting level (5) Block of SD by excess extracellular chloride (6) Annihilation of two SD waves that collide head on (7) Multiple waves in response to a suprathreshold (sustained) stimulus (8) Waves of increased K^+ of approximately the correct amplitude in both normal and TTX treated cortex (9) An SD wave whose K^+ amplitude is about the same as that measured in rat cortex, travelling with a velocity of 2.9 mm/min in comparison with the experimental velocity of 3 mm/min (10) SD may be sometimes very difficult to elicit and sometimes impossible (11) Neuronal and glial depolarization during SD (12) Increased rate of spiking of neurons ahead and behind the SD wave peak (13) K^+ waves which may either have a monotonically decreasing tail or have a tail which has a secondary peak (14) A linear relation between the velocity and the amplitude of the K^+-wave.

The model thus has a considerable number of successes in predicting experimental phenomena associated with SD. Some aspects of SD are not addressed by the model, for example, the surface potential and the EEG activity during SD. The glial depolarization of course follows immediately from the fact that glial membrane potential is closely V_K. The increase in firing rate of neurons at the start and cessation of the entry of an SD wave into their neighborhood has more or less been "built into" the model.

The model predictions of the velocity of SD are a stringent test. The most successful comparison was listed in (9) above where the most information was known about the K^+ wave. In other cases where the experimental data was not so complete, the agreement between predicted and observed velocity was not so good but still reasonable. In one case (cat cerebellum) the model prediction and the experimentally reported velocity differed widely, but the experimental velocity was not measured directly and further experimentation is necessary before this can be called a failure of the model. If it eventuates that the velocity in this preparation is as high as reported, then the model would have to be modified to include other factors which would make the SD wave travel faster.

One other set of experimental data cannot be immediately compared with model results. This is the block of SD by divalent cations (Bures *et al.*, 1974). This is not to be cast as a failure of the model. The manner in which divalent cations block SD is believed via an interference with ion conductances. To model these effects would require a consideration of individual ion channels and possibly receptor molecules. A phenomenological approach could also be adopted. For example, one could make the presynaptic calcium conductance a decreasing function of Mg^{++} concentration which would lead to a block of SD by elevated external magnesium ion concentration.

Generally speaking, the model does seem to predict most of the qualitative effects observed in SD and to a lesser extent quantitative aspects as well. The wave amplitude's dependence on depth

in the cortex has not been incorporated in the model equations. This would not be theoretically difficult but it would be computationally time consuming. To illustrate the kind of change that would have to be made, consider the equation for $K^o = K^o(x, z, t)$, for example, where z is the depth in the cortex. We would then have

$$\frac{\partial K^o}{\partial t} = D_K\left(\frac{\partial^2 K^o}{\partial x^2} + \frac{\partial^2 K^o}{\partial z^2}\right) + F(\mathbf{C}, z), \quad (27)$$

where now the source terms depend on depth. The qualitative behavior of the resulting system of equations would be the same as that without z-dependence but now the amplitude of the wave would depend on z. Similarly the reverberating SD experiments of Shibata and Bures (1972, 1974) could be studied theoretically using the appropriate geometry and boundary conditions with a $K^o = K^o(x, y, t)$ equation modified to

$$\frac{\partial K^o}{\partial t} = D_K\left(\frac{\partial^2 K^o}{\partial x^2} + \frac{\partial^2 K^o)}{\partial y^2}\right) + F(\mathbf{C}), \quad (28)$$

where x and y are coordinates in the plane of the cortical surface. The z-dependence could also be included but is not necessary to show the phenomenon of reverberation around closed loop pathways. In all these cases where extra space dimensions are included, there is necessarily a very large increase in the amount of computation needed to obtain numerical solutions of the equations.

Some of the parameters and constants of the model studied in this paper are reasonably well known, based on experiments on various preparations but not usually on data from cortical cells. The constants k_1, k_2, k_4, k_5 and c which determine the actual magnitudes of the source and sink terms for K^+ and Ca^{++} are not known. These have been estimated by ensuring that the model system of equations has solutions which are close to those observed experimentally in SD. Unfortunately, it seems that measurement which would lead to a knowledge of these constants does not seem feasible. For example, it seems that it would be very difficult to measure the presynaptic calcium conductance of cortical cells or the number density and strength of individual K^+ or Ca^{++} pump sites. Despite the lack of an accurate method of assessing the values of such constants, it is felt that a coupled system of reaction diffusion equations whose components are the ion and transmitter concentrations, constitutes a plausible basis for a theory of spreading depression.

REFERENCES

Blinkov, S. M. & Glezer, I. I. *The Human Brain in Figures and Tables.* New York: Plenum, 1968.

Brinley, F. J., Jr. Ion fluxes in the central nervous system. *International Review of Neurobiology*, 1963, **5**, 183–242.

Brinley, F. J., Jr., Kandel, E. R., & Marshall, W. H. Potassium outflux from rabbit cortex during spreading depression. *Journal of Neurophysiology*, 1960, **23**, 246–256.

Bures, J., Buresova, O., & Krivanek, J. *The Mechanism and Application of Leao's Spreading Depression of Electroencephalographic Activity.* New York: Academic Press, 1974.

Calvin, W. H. Generation of spike trains in CNS neurons. *Brain Research*, 1975, **84**, 1–22.

Campbell, C. W. B. The Na^+, K^+, Cl^- contents and derived membrane potentials of presynaptic nerve endings in vitro. *Brain Research*, 1976, **101**, 594–599.

Eccles, J. C., Llinas, R., & Sasaki, K. Parallel fiber stimulation and the responses induced thereby in the Purkinje cells of the cerebellum. *Experimental Brain Research*, 1966, **1**, 17–39.

Goldensohn, E. S. & Walsh, G. S. Sequential functional changes in single cortical neurons during spreading depression. *EEG Clinical Neurophysiology*, 1968, **24**, 290–291.

Grafstein, B. Mechanism of spreading cortical depression. *Journal of Neurophysiology*, 1956, **19**, 154–171.

Grafstein, B. Neuronal release of potassium during spreading depression. In: *Brain Function*, Vol. I, M. A. B. Brazier (Ed.), Berkeley: University of California Press, 1963.

Higashida, H., Mitarai, G., & Watanabe, S. A comparative study of membrane potential changes in neurons and neuroglial cells during spreading depression in the rabbit. *Brain Research*, 1974, **65**, 411–425.

Hodgkin, A. L. & Huxley, A. F. A quantitative description of membrane current and its application to conduction and excitation in nerve. *Journal of Physiology (London)*, 1952, **117**, 500–544.

Hodgkin, A. L. & Katz, B. The effect of sodium ions on the electrical activity of the giant axon of the squid. *Journal of Physiology (London)*, 1949, **108**, 37–77.

Kraig, R. P. & Nicholson, C. Extracellular ionic variations during spreading depression. *Neuroscience*, 1978, **3**, 1045–1059.

Krivanek, J. & Bures, J. Ion shifts during Leao's spreading cortical depression. *Physiol. Bohemoslov.*, 1960, **9**, 494–503.

Leao, A. A. P. Spreading depression of activity in the cerebral cortex. *Journal of Neurophysiology*, 1944, **7**, 359–390.

Lees, M. In: *Numerical Solution of Partial Differential Equations*, Ames, W. F. (Ed.). New York: Barnes and Noble, 1969.

Llinas, R., Steinberg, I. Z., & Walton, K. Presynaptic calcium currents and their relation to synaptic transmission; voltage clamp study in squid giant synapse and theoretical model of the calcium gate. *Proceedings of the National Academy of Science, U.S.A.*, 1976, **73**, 2918–2922.

Mayevsky, A. & Chance, B. Repetitive patterns of metabolic changes during cortical spreading depression of the awake rat. *Brain Research*, 1974, **65**, 529–533.

Nicholson, C., Ten Bruggencate, G., Steinberg, R., & Stockle, H. Calcium modulation in brain extracellular microenvironment demonstrated with ion-selective micropipette. *Proceedings of the National Academy of Science, U.S.A.*, 1977, **74**, 1287–1290.

Nicholson, C., Ten Bruggencate, G., Stockle, H., & Steinberg, R. Calcium and potassium changes in extracellular microenvironment of cat cerebellar cortex. *Journal of Neurophysiology*, 1978, **41**, 1026–1039.

Ochs, S. The nature of spreading depression in neural networks. *International Review of Neurobiology*, 1962, **4**, 1–69.

Quastel, D. M. J. Excitation-secretion coupling at the mammalian neuromuscular junction. In: *Synaptic Transmission and Neuronal Interaction*, p. 23. New York: Raven Press, 1974.

Sachs, J. R. Kinetics of the inhibition of the Na-K pump by external sodium. *Journal of Physiology (London)*, 1977, **264**, 449–467.

Shibata, M. & Bures, J. Reverberation of cortical spreading depression along closed-loop pathway in the rat cerebral cortex. *Journal of Neurophysiology*, 1972, **35**, 381–388.

Shibata, M. & Bures, J. Optimum topographical conditions for reverberating cortical spreading depression in rats. *Journal of Neurobiology*, 1974, **5**, 107–118.

Sugaya, E., Takato, M., & Noda, Y. Neuronal and glial activity during spreading depression in the cerebral cortex of cat. *Journal of Neurophysiology*, 1975, **38**, 822–841.

Tuckwell, H. C. Solitons in reaction-diffusion system. *Science*, 1979, **205**, 493–495.

Tuckwell, H. C. & Miura, R. M. A mathematical model for spreading cortical depression. *Biophysical Journal*, 1978, **23**, 257–276.

Van Harreveld, A. & Fifkova, E. Mechanisms involved in spreading depression. *Journal of Neurobiology*, 1973, **4**, 375–387.

Vyskocil, F., Kriz, N., & Bures, J. Potassium-selective microelectrodes used for measuring the extracellular brain potassium during spreading depression and anoxic depolarization in rats. *Brain Research*, 1972, **39**, 255–259.

Wilson, H. R. & Cowan, J. D. A mathematical theory of the functional dynamics of cortical and thalamic nervous tissue. *Kybernetik*, 1973, **13**, 55–80.

Reference Notes

Tuckwell, H. C. Simplified reaction-diffusion equations for spreading cortical depression. Unpublished ms.